Performance Optimization of ZnS/CIGS Solar Cell With Over 25% Efficiency Enabled by Using a $CuIn_3Se_5$ OVC Layer

Md. Billal Hosen*, Md. Karamot Ali*, Md. Asaduzzaman*, Abu Kowsar**‡, Ali Newaz Bahar*, ***

*Department of ICT, Mawlana Bhashani Science and Technology University, Tangail - 1902, Bangladesh.

**Institute of Fuel Research and Development (IFRD), Bangladesh Council of Scientific and Industrial Research (BCSIR), Dhaka-1205, Bangladesh

***Department of Electrical and Computer Engineering, University of Saskatchewan, SK, Canada.

(ali.bahar@usask.ca, apukowsar@gmail.com)

‡Corresponding Author; Abu Kowsar, Institute of Fuel Research and Development (IFRD), Bangladesh Council of Scientific and Industrial Research (BCSIR), Dhanmondi, Dhaka-1205, Tel: +88 01722281618, apukowsar@gmail.com

Received: 11.10.2020 Accepted:25.11.2020

Abstract- Chalcopyrite CIGS solar cells have been demonstrated with the highest efficiency for thin-film solar cell families. Herein, the effects of thickness and bandgap of cadmium (Cd) free ZnS buffer layer grown on CIGS absorber with an ordered vacancy compound (OVC) at buffer/absorber interface in CIGS solar cell structure have been investigated using ADEPT 2.1 simulator. The ZnS buffer possesses a wider energy bandgap than the traditional CdS buffer layer, which substantiates the higher conversion efficiency of this solar cell, allowing the photons of lower wavelength into the CIGS layer. Besides, $CuIn_3Se_5$ has been used as an OVC layer that assists to improve the conversion efficiency to an optimized level of over 25% by reducing the recombination rate. Moreover, the optimized short circuit current (J_{sc}) and corresponding open-circuit voltage (V_{oc}) yield a higher fill factor (FF) of 86.22%, which, therefore, results in an optimum efficiency of the CIGS cell estimated as 25.68% under AM 1.5 irradiance.

Keywords CIGS solar cell, thin-film, Cd-free, ZnS buffer, OVC, efficiency.

1. Introduction

Polycrystalline CIGS solar cell has drawn much attention in recent years because of its high efficiency and comparatively lower fabrication cost [1-3]. To date, Solar Frontier developed the highest efficiency for these solar cells, recorded as 22.9% with the CdS buffer layer [4] and recorded as 23.35% with the Cd-free buffer layer [5, 6]. The standard device structure of CIGS based solar cells is comprised of SLG/Mo/CIGS (absorber)/CdS buffer layer/undoped ZnO/ZnO:Al stack. The buffer layer in this stack ensures better optical transparency and electrical interface between the transparent ZnO window and the CIGS absorber layer. Historically, chemical bath deposited (CBD) cadmium sulfide (CdS) of 2.42 eV is being employed as a buffer layer in the CIGS device structure [7]. However, the direct bandgap CdS causes parasitical absorption in the shorter wavelength region and results in the fall of quantum efficiency [8]. Another disadvantage is that the cadmium (Cd) is carcinogenic and toxic in nature, which is deleterious for the environment as well as for almost all creatures [9]. Furthermore, the non-vacuum CBD process is deleterious for the vacuum line as the ZnO window layer, and the CIGS absorber layers are usually deposited using vacuum-based RF sputtering and co-evaporation technique, respectively [10]. For the reasons mentioned earlier, the development of the Cd-free substitute buffer layer materials and the employment of other growth techniques instead of conventional CBD have drawn attention among the researchers [11].

In this work, we have designed and optimized a novel combination of CIGS solar cells incorporating the $CuIn_3Se_5$ OVC layer and simulated the efficiency of the cell, and analyzed the effects of ZnS buffer layer thickness and bandgap on these cells using ADEPT 2.1 simulator. Eventually, we studied the performance of the proposed Cd-free CIGS structure due to the change in thickness of the OVC layer and then compared it to the performance of the CIGS module, having a CdS buffer layer and found significant enhancement of the conversion efficiency. To the best of our knowledge, there is no such type of work reported in literature.

The frequently used terms have been presented in the following Table 1.

Table 1. Acronym and nomenclature of the frequently used terms.

Acronym	Nomenclature
CIGS	Copper Indium Gallium Selenide
OVC	Ordered Vacancy Compound
$CuIn_3Se_5$	Copper Indium Selenide
ADEPT	A Device Emulation Program and Tool
AMPS	Analysis of Microelectronic and Photonic Structures
SCAPS	Solar Cell Capacitance Simulator
CdS	Cadmium Sulfide
ZnS	Zinc Sulfide
ZnO: Al	Aluminum-Doped Zinc Oxide
i-ZnO	Intrinsic Zinc Oxide
SLG	Soda Lime Glass
FF	Fill-Factor

2. Methodology

2.1. Proposed Design of CIGS Solar Cell

It is conceived that for CIGS solar cells, the bandgap of the buffer layer should be wider, and the electron affinity should be lower compared to that of CIGS absorber when the recombination occurs at the interface. We choose a direct bandgap ZnS ternary alloy of 2.60 eV as an alternative buffer layer material of widely used CdS [25, 26]. It overcomes the state of parasitic absorption due to having a wider bandgap with a lower electron affinity. The direct bandgap of CdS (2.42 eV) corresponding to the wavelength of around 520 nm is not adequate to transmit the light with a shorter wavelength to the absorber. Since the bandgap of ZnS is so wider than CdS, the more photons will be transmitted to the absorber that therefore enhances this cell quantum efficiency. A schematic design of this solar cell is shown in Fig. 1.

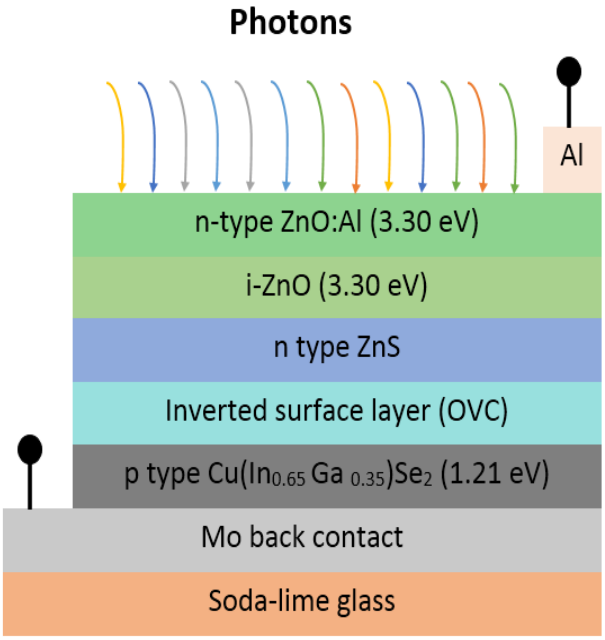

Fig. 1. A schematic device structure for CIGS solar cell.

It has been earlier mentioned that the non-toxic ZnS has been proposed as an active buffer layer. A highly resistive semiconductor material, intrinsic zinc oxide (i-ZnO) was sandwiched between the conductive aluminum-doped zinc oxide (ZnO: Al) window layer and the ZnS buffer layer. Aluminum (Al) grids were used as the front contact electrode and Molybdenum (Mo) as a back contact electrode. The bandgap profile for the entire cell has been depicted in Fig. 2.

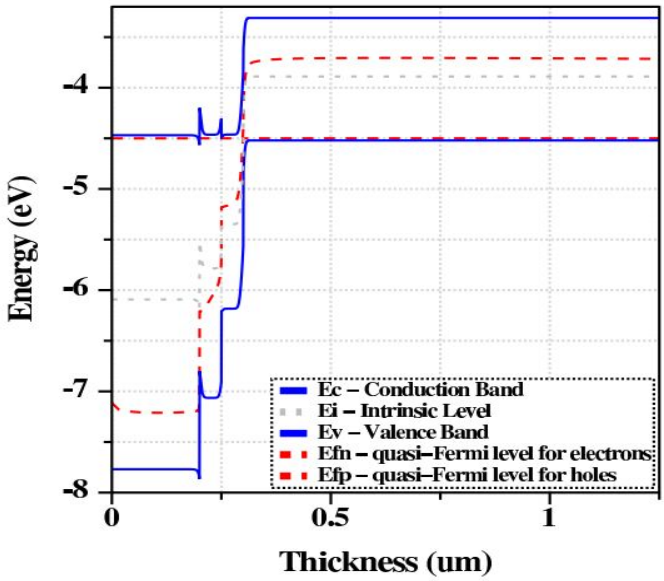

Fig. 2. Bandgap profile for the entire CIGS cell.

2.2. Simulation Approach

In this work, a numerical simulation was carried out by widely used ADEPT 2.1 (A Device Emulation Program and Tool), an online-based device simulator [12]. This simulation tool has been widely used for modeling solar cells consist of a variety of thin-film semiconductor materials like AMPS-1D, SCAPS-1D, MSCS-1D etc. [21]. The simulation was performed using the major input optoelectronic parameters of different layers of the cell at a temperature of 300*K*. These parameters have been presented in Table 2. These default values are picked out from several experimental photovoltaic research works based on the materials used in different thin-film photovoltaic devices [11, 13-18, 24].

Performance parameters such as the short circuit current density (J_{sc}), open-circuit voltage (V_{oc}), fill factor (FF), and efficiency (η) of the completed photovoltaic cell were simulated from the J-V characteristics curve and the output log after conveying the simulation. Here the temperature and the shadowing factor were kept at 300*K* and 10%, respectively. The simulation was performed using the default values, as described in Table 3. After that, the performances were measured and optimized by varying thickness and doping concentration of different layers.

Table 2. Symbolic representation of material properties [22]

Parameters	Symbols	Units
Thickness	τ	μm
Dielectric constant	K_s	Constant
Refractive index	N_{dx}	Constant
Bandgap	E_g	eV
Electron affinity	χ_e	eV
Electron mobility	μ_n	$cm^2\ V^{-1}s^{-1}$
Hole mobility	μ_p	$cm^2\ V^{-1}s^{-1}$
Conduction band effective density of states	N_c	cm^{-3}
Valence band effective density of states	N_v	cm^{-3}
Donor concentration	N_d	cm^{-3}
Acceptor concentration	N_a	cm^{-3}
Electron lifetime	t_n	sec
Hole lifetime	t_p	sec
Short circuit current density	J_{sc}	mA/cm^2
Open-circuit voltage	V_{oc}	V
Efficiency	η	%

Table 3. Optoelectronic parameters of different layers at a temperature of 300*K*.

Parameters	ZnO:Al [18]	i-ZnO [16, 18]	ZnS [22]	OVC [23]	CIGS [16]
τ	0.2	0.02	0.05	0.05	1
K_s	7.8	7.8	12	13.28	13.6
N_{dx}	2	2	3.15	3.67	3.67
E_g	3.3	3.3	2.6	1.72	1.21
χ_e	4.6	4.6	3.74		4.21
μ_n	100	60	200	40	100
μ_p	30	20	40	10	25
N_c	2.2×10^{18}	2.2×10^{18}	2.2×10^{18}	1.7×10^{19}	2.2×10^{18}
N_v	1.8×10^{19}	1.8×10^{19}	1.8×10^{19}	2.4×10^{18}	1.8×10^{19}
N_d	1×10^{16}	2×10^{16}	1×10^{16}	5×10^{18}	0
N_a	0	0	0	0	5×10^{15}
t_n	5×10^{-8}	6×10^{-8}	2×10^{-8}	2×10^{-8}	1×10^{-8}
t_p	5×10^{-9}	4×10^{-9}	6×10^{-8}	6×10^{-8}	5×10^{-8}

3. Result Analysis and Discussion

3.1. Performance variation due to substitute ZnS buffer layer

From the simulation, it is evident that the ZnS buffer layer plays a significant role in increasing efficiency. Owing to the wider bandgap, ZnS increased the reverse saturation current that increased the Voc dramatically, therefore resulted in an increase of the overall CIGS cell efficiency. This improvement appeared for the sake of a large number of photons transmitted into the absorber. The photons having low wavelengths are also transmitted into the CIGS layer due to the higher bandgap of ZnS than of CdS. Additionally, the interface defect density at the ZnS/CIGS interface was devoted to 1×10^{10} cm^{-2}. To demonstrate the performance of the cell, we also analyzed the effects of thickness and doping concentration that is shown in Fig. 3. The simulations considered the radiant power of incident light with 1000 Wm^{-2} for airmass AM1.5G under 1 sun condition. By studying the results, the thickness for the ZnS buffer was optimized as 0.06 μm, whereas the optimum doping concentration was 5×10^{16} cm^{-3}. This optimized thickness

results in a defect field that is very small in amount as the critical layer thickness for the ZnS buffer is 0.034 μm and hence contributes to aggrade the cell performance.

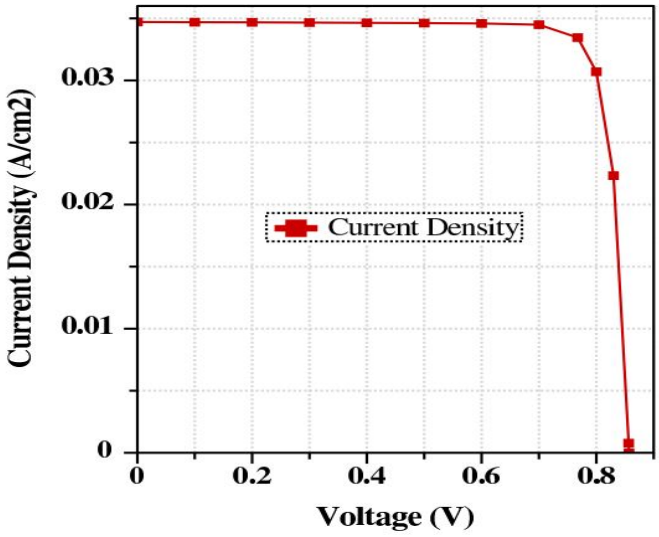

Fig. 3. J-V characteristics curve of CIGS cell with ZnS buffer.

However, a higher doping density is possible for the n-type ZnS buffer. In the space-charge region, it lifts the electric field and thus enhances the drift velocity of the electrons in both buffer and absorber layers. The output current is also increased due to this enhancement drift velocity. Concurrently, the heavily doped buffer increases the hole recombination rate, which in turn, degrades the output current. Eventually, this alteration in output current relies upon which of these different constituents prevails at a specific doping concentration. The efficiency is increased to a level of 22.07% after optimizing the values of these parameters.

3.2. Effects of OVC layer on cell performance

It has been observed that the OVC semiconductor material $CuIn_3Se_5$ shows strong photoconductive nature [19]. The use of the OVC layer in solar cells inhibits interface states between the absorber and window layer, and the cell provides more prominent efficiency owing to having OVC [20]. The simulated efficiency has been increased as the FF increases along with the increase of V_{oc} due to negative space charge at the ZnS/CIGS interface. As discussed earlier, while using ZnS as a buffer layer along with OVC at the ZnS/CIGS interface in the device, the efficiency of the CIGS solar cell reaches the maximal level. In this high efficacy cell, the voltage (Vm) and current density (Jm) at maximum power point were obtained as 767.96 mV and 33.44mA/cm^2, respectively. And the Voc and J_{sc} were simulated as 856.93 mV and 34.75 mAcm^{-2}, respectively. These values result in a fill factor of 86.22%, which yields an efficiency of 25.68%. The J-V characteristics curve for the optimized cell has been pictured in Fig. 4.

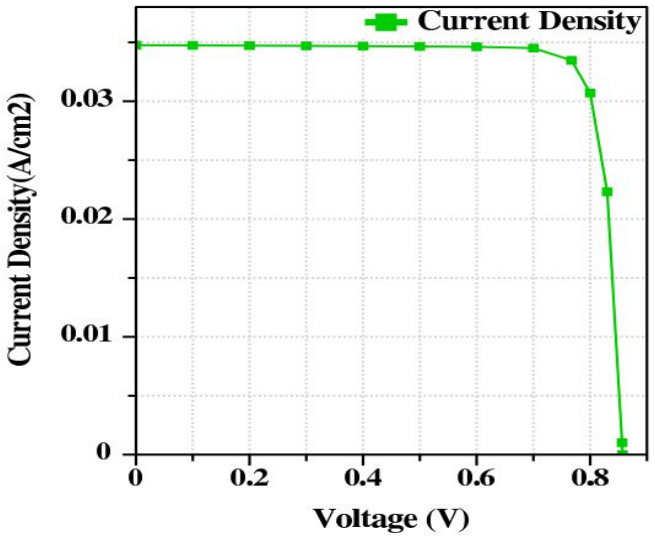

Fig. 4. J-V characteristics curve for the optimized CIGS cell.

Finally, the comparison between the performance of the proposed CIGS solar cell and the previous record cell has been demonstrated in Table 4.

Table 4. Current density-voltage data of the proposed device compared to the previous champion CIGS solar cell with record efficiency.

Description	V_{oc} (mV)	J_{sc} (mAcm^{-2})	FF (%)	η (%)
Previous record with Cd-free buffer layer [5]	734	39.6	80.4	23.35
Proposed cell with Cd-free ZnS buffer layer	782.60	35.19	80.12	22.07
Proposed cell with ZnS buffer layer and OVC	856.93	34.75	86.22	25.68

From Table 4, it is apparent that the energy conversion efficiency of the proposed cell with the ZnS buffer layer and OVC is about 2.33% more than the previous record efficiency with the Cd-free buffer layer. Moreover, the fill

factor of the cell is improved to a level of 86.22% because of the increased V_{oc} and its corresponding J_{sc}.

4. Conclusion

In the paper, a new combination of CIGS solar cell structure has been optimized with a 25.7% theoretical efficiency. A ZnS buffer layer having a bandgap of 2.6 eV wider than of the conventional CdS has been employed in this CIGS cell along with the $CuIn_3Se_5$ OVC layer. The minimum defect density, lattice mismatch, and crystallographic disorder substantiate the hetero-epitaxial growth of ZnS buffer with the OVC layer on the CIGS absorber. To make the fabrication process more cost-effective, the thicknesses of all layers were kept near about the critical thicknesses. Finally, it is proposed that ZnS would be a promising substitute for the CdS buffer layer for high efficiency, environment-friendly CIGS ultra-thin film solar cells.

Acknowledgments

The authors of this paper would like to acknowledge to the Department of ICT, Mawlana Bhashani Science and Technology University for technical supports. This work was financially supported by Bangladesh Council of Scientific and Industrial Research (BCSIR) regular R&D Scope (Ref. no: 39.02.0000.011.14.111.2019/228; Serial No. 41; Date: 06.11.2019).

References

[1] K. Kim, I. Jeong, Y. Cho, D. Shin, S. Song, S. K. Ahn, Y.-J.Eo, A.Cho, C. Jung, W. Jo, J. H. Kim, P. P. Choi, J. Gwak, J. H. Yun, "Mechanisms of extrinsic alkali incorporation in CIGS solar cells on flexible polyimide elucidated by nanoscale and quantitative analyses," Nano Energy, vol. 67, p. 104201, 2020.

[2] A. Kowsar, S. F. U. Farhad, M. Rahaman, M. S. Islam, A. Y. Imam, S. C. Debnath, "Progress in major thin-film solar cells: Growth technologies, layer materials and efficiencies," International Journal of Renewable Energy Research (IJRER), vol. 9, pp. 579-597, 2019.

[3] J. Lindahl, J. Keller, O. Donzel-Gargand, P. Szaniawski, M. Edoff, and T. Törndahl, "Deposition temperature induced conduction band changes in zinc tin oxide buffer layers for Cu (In, Ga) Se2 solar cells," Solar Energy Materials and Solar Cells, vol. 144, pp. 684-690, 2016.

[4] T. Kato, J.-L. Wu, Y. Hirai, H. Sugimoto, and V. Bermudez, "Record efficiency for thin-film polycrystalline solar cells up to 22.9% achieved by Cs-treated Cu (In, Ga)(Se, S) 2," IEEE Journal of Photovoltaics, vol. 9, pp. 325-330, 2018.

[5] M. Nakamura, K. Yamaguchi, Y. Kimoto, Y. Yasaki, T. Kato, and H. Sugimoto, "Cd-free Cu (In, Ga)(Se, S) 2 thin-film solar cell with record efficiency of 23.35%," IEEE Journal of Photovoltaics, vol. 9, pp. 1863-1867, 2019.

[6] M. A. Green, E. D. Dunlop, J. Hohl-Ebinger, M. Yoshita, N. Kopidakis, and A. W. Ho-Baillie, "Solar cell efficiency tables (Version 55)," Progress in Photovoltaics: Research and Applications, vol. 28, pp. 3-15, 2020.

[7] R. Bhattacharya and K. Ramanathan, "Cu (In, Ga) Se2 thin film solar cells with buffer layer alternative to CdS," Solar Energy, vol. 77, pp. 679-683, 2004.

[8] M. Asaduzzaman, M. Hasan, and A. N. Bahar, "An investigation into the effects of band gap and doping concentration on Cu (In, Ga) Se 2 solar cell efficiency," SpringerPlus, vol. 5, p. 578, 2016.

[9] M. P. Waalkes, "Cadmium carcinogenesis," Mutation Research/Fundamental and Molecular Mechanisms of Mutagenesis, vol. 533, pp. 107-120, 2003.

[10] D. Hariskos, S. Spiering, and M. Powalla, "Buffer layers in Cu (In, Ga) Se2 solar cells and modules," Thin Solid Films, vol. 480, pp. 99-109, 2005.

[11] N. Naghavi, D. Abou-Ras, N. Allsop, N. Barreau, S. Bücheler, A. Ennaoui, et al., "Buffer layers and transparent conducting oxides for chalcopyrite Cu (In, Ga)(S, Se) 2 based thin film photovoltaics: present status and current developments," Progress in Photovoltaics: Research and Applications, vol. 18, pp. 411-433, 2010.

[12] J. Gray, X. Wang, R. V. K. Chavali, X. Sun, A. Kanti, and J. R. Wilcox, "ADEPT 2.1," 2011.

[13] O. Lundberg, M. Bodegård, J. Malmström, and L. Stolt, "Influence of the Cu (In, Ga) Se2 thickness and Ga grading on solar cell performance," Progress in Photovoltaics: Research and Applications, vol. 11, pp. 77-88, 2003.

[14] S. H. Song and S. A. Campbell, "Heteroepitaxy and the performance of CIGS solar cells," in 2013 IEEE 39th Photovoltaic Specialists Conference (PVSC), 2013, pp. 2534-2539.

[15] K. E. Haque and M. M. H. Galib, "An investigation into III–V compounds to reach 20% efficiency with minimum cell Thickness in ultrathin-film solar cells," Journal of electronic materials, vol. 42, pp. 2867-2875, 2013.

[16] P. Chelvanathan, M. I. Hossain, and N. Amin, "Performance analysis of copper–indium–gallium–diselenide (CIGS) solar cells with various buffer layers by SCAPS," Current Applied Physics, vol. 10, pp. S387-S391, 2010.

[17] E. Schlenker, V. Mertens, J. Parisi, R. Reineke-Koch, and M. Köntges, "Schottky contact analysis of photovoltaic chalcopyrite thin film absorbers," Physics Letters A, vol. 362, pp. 229-233, 2007.

[18] M. Asaduzzaman, A. N. Bahar, M. M. Masum, and M. M. Hasan, "Cadmium free high efficiency Cu2ZnSn (S, Se) 4 solar cell with Zn1− xSnxOy buffer layer," Alexandria engineering journal, vol. 56, pp. 225-229, 2017.

[19] H. Wang, I. Shih, and C. Champness, "Studies on monocrystalline CuInSe2 and CuIn3Se5," Thin Solid Films, vol. 361, pp. 494-497, 2000.

[20] S. H. Kwon, S. C. Park, B. T. Ahn, K. H. Yoon, and J. Song, "Effect of CuIn3Se5 layer thickness on CuInSe2 thin films and devices," Solar Energy, vol. 64, pp. 55-60, 1998.

[21] A. Belkaid, I. Colak, K. Kayisli, M. Sara, R. Bayindir, "Modeling and Simulation of Polycrystalline Silicon Photovoltaic Cells", 7th International Conference on Smart Grid (icSmartGrid), 2019.

[22] S. M. Sze and K. K. Ng, Physics of Semiconductor Devices: John wiley & sons, 2006.

[23] R. Jacob, R. Geethu, T. Shripathi, G. S. Okram, V. Ganesan, B. Pradeep, R. R. Philip, "Optoelectronic and low temperature thermoelectric effects in the OVC n-$CuIn_3Se_5$ thin films", Physica Status Solidi (a), 209(11), 2195–2200, 2012.

[24] A. Parisi, L. Curcio, V. Rocca, S. Stivala, A. C. Cino, A. C. Busacca, G. Cipria, "Photovoltaic module characteristics from CIGS solar cell modelling", International Conference on Renewable Energy Research and Applications (ICRERA), 2013.

[25] S. Akhanda, R. Matin, M. S. Bashar, M. Sultana, A. Kowsar, M. Rahaman, Z. H. Mahmood, **"**Effect of annealing atmosphere on structural and optical properties of CZTS thin films prepared by spin-coating", Bangladesh Journal of Scientific and Industrial Research (BJSIR), 53(1):13, 2018.

[26] S. Akhanda, R. Matin, M. S. Bashar, A. Kowsar**,** M. Rahaman, Z. H. Mahmood,"Experimental Study on Structural, Optical and Electrical Properties of Chemical Bath Deposited CdZnS Thin Films", Journal of Fundamentals of Renewable Energy and Applications, Vol 7(1), 2017.